AJNR

Assessment of White Matter Damage in Subacute Sclerosing Panencephalitis Using Quantitative Diffusion Tensor MR Imaging

R. Trivedi, R.K. Gupta, A. Agarawal, K.M. Hasan, A. Gupta, K.N. Prasad, G. Bayu, D. Rathore, R.K.S. Rathore and P.A. Narayana

AJNR Am J Neuroradiol 2006, 27 (8) 1712-1716
http://www.ajnr.org/content/27/8/1712

ORIGINAL RESEARCH

Assessment of White Matter Damage in Subacute Sclerosing Panencephalitis Using Quantitative Diffusion Tensor MR Imaging

R. Trivedi
R.K. Gupta
A. Agarawal
K.M. Hasan
A. Gupta
K.N. Prasad
G. Bayu
D. Rathore
R.K.S. Rathore
P.A. Narayana

BACKGROUND AND PURPOSE: Subacute sclerosing panencephalitis (SSPE), a rare progressive degenerative disease, is caused by persistent infection with a defective measles virus. The correlation between the clinical staging and MR imaging is usually poor. The aim of the study was to investigate the role of diffusion tensor imaging (DTI) in the early detection of white matter damage in SSPE in the presence of normal findings on conventional imaging.

METHODS: DTI was performed in 21 patients in stage II SSPE and 10 age/sex-matched healthy controls. Fractional anisotropy (FA) and mean diffusivity (MD) values were calculated in the periventricular white matter, corpus callosum, and posterior limb of the internal capsule in patients with normal and abnormal findings on conventional imaging as well as healthy controls.

RESULTS: The patients were grouped into those with normal ($n = 11$) and abnormal ($n = 10$) findings on conventional imaging for the purpose of quantitative DTI analysis. Abnormal- and normal-appearing white matter on T2-weighted images showed significantly decreased FA values in all the regions compared with those in healthy controls. MD values were significantly increased in the periventricular white matter region of the frontal and parietooccipital lobe in patients with normal as well as abnormal findings on conventional imaging compared with those in healthy controls.

CONCLUSION: DTI detects early white matter abnormalities that may have significant therapeutic implication, even in the presence of normal findings on conventional imaging, in patients with SSPE.

Subacute sclerosing panencephalitis (SSPE) results from a slow viral infection of the central nervous system secondary to measles. The annual incidence rate varies from 1 to 4 per million population in developed countries; however, in the developing countries, this could be as high as 21 per million population.[1] Most patients have a history of measles infection at an age younger than 2 years.[2] Symptoms of SSPE usually appear after a latent period of approximately 6–8 years of clinical measles infection.[3] Diagnosis of SSPE is usually based on typical clinical and electroencephalography (EEG) findings and demonstration of a high titer of measles antibody in the CSF.[4] Early symptoms of SSPE are mild intellectual deterioration followed by the onset of myoclonus, convulsions, and abnormal postures and movements, progressing to optic atrophy, motor weakness, and akinetic mutism and ending in coma and death.[2]

Most of the information regarding the histopathology of SSPE is available only in the late stage of the disease, either at autopsy or by cortical biopsies that show astrogliosis, neuronal loss and degeneration, demyelination, neurofibrillary tangles, and infiltration of inflammatory cells.[5-9] Occipital lobe biopsy from 2 patients with clinical stage II SSPE showed the presence of inclusion bodies along with nonspecific findings of encephalitis.[5]

In the early stages of disease, findings of brain imaging studies are usually negative, though MR imaging is more sensitive than CT for lesion detection.[10,11] Recently, metabolite abnormalities in the normal-appearing white matter (NAWM) of patients with SSPE have been described on in vivo proton MR spectroscopy,[3,12]

Diffusion tensor imaging (DTI) is shown to be valuable in studies of neuroanatomy, compact white matter fiber connectivity,[13] and brain development.[14] The aim of our study was to investigate the role of quantitative DTI in patients with SSPE in defining the microstructural damage that may have significant therapeutic implication in patients with normal findings on conventional MR imaging.

Materials and Methods

We describe 21 children with SSPE (14 boys and 7 girls) with a mean age of 8.6 years (range, 5–14 years). All patients were consistent right-handers. The diagnosis of SSPE was based on typical clinical presentation, EEG pattern, and elevated CSF anti-measles antibody titer.[4] The characteristic EEG pattern was suppression burst episodes, in which high-amplitude slow and sharp waves of 3–5 seconds recur at intervals of 5 to 8 seconds on a slow background in all these cases. Passive particulate agglutination test (Serodia-Measle; Fujirebio, Tokyo, Japan) for the detection and titration of antibodies to measles virus was used. CSF antibody titer ≥1:128 was considered positive for measles virus infection. The age at measles infection, which could be ascertained in 14 children, ranged from 6 months to 2 years in 13 children and at age 4 years in the remaining child. There was a mean latent period of 7.6 years (range, 4–11 years) for the onset of clinical symptoms in patients with a history of measles. There was a mean gap of 5.8 months (range, 2–12 months) between the onset of symptoms and the imaging in all these cases.

Received November 14, 2005; accepted after revision December 12.

From the Department of Radiodiagnosis (R.T., R.K.G., A.G.) and Microbiology (K.N.P.), Sanjay Gandhi Post Graduate Institute of Medical Sciences, Lucknow, UP, India; the Department of Neurology (A.A.), King George Medical University, Lucknow, UP, India; the Department of Mathematics (G.B., D.R., R.K.S.R.), Indian Institute of Technology, Kanpur, UP, India; and the Department of Diagnostic and Interventional Imaging (K.M.H., P.A.N.), University of Texas Medical School at Houston, Houston, Tex.

Richa Trivedi received financial assistance from the Council of Scientific and Industrial Research, New Delhi, India.

Please address correspondence to Rakesh K. Gupta, MD, MR Section, Department of Radiodiagnosis, Sanjay Gandhi Post Graduate Institute of Medical Sciences, Lucknow, UP, India 226014; e-mail: rakeshree@hotmail.com; rgupta@sgpgi.ac.in

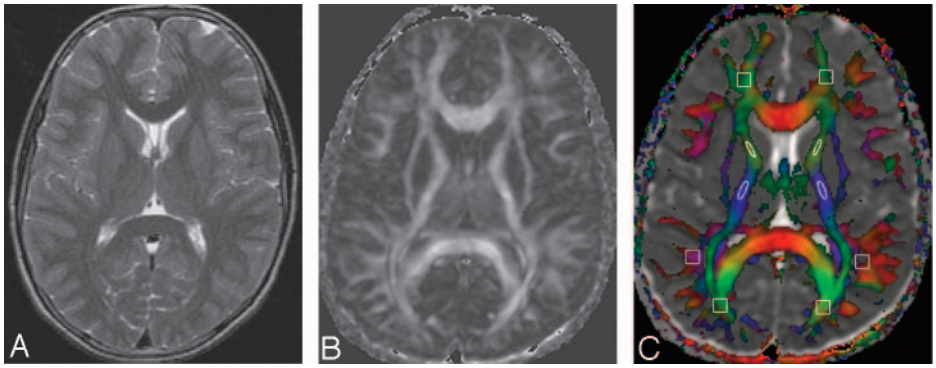

Fig 1. A 6-year-old healthy control. T2-weighted (*A*), FA (*B*), and color-coded FA images fused with apparent diffusion coefficient (ADC) maps (*C*) through the lateral ventricles show normal distribution of white matter. The rectangular and elliptic ROIs are placed (*C*) on the frontal, parietal, and occipital cerebral lobes and the posterior limb of the internal capsule for quantification of FA and MD values. The cutoff value for the color-coded FA for display is kept at 0.2 (*C*), above which the color-coded regions reflect the white matter only (red [right–left)], green [anteroposterior], and blue [superior–inferior)]).

The usual clinical presentation was myoclonus, altered behavior, and cognitive decline. In addition, 12 of the 21 children had extrapyramidal symptoms and difficulty in walking. Jabbour et al[4] classified these children with SSPE into the following 4 stages on the basis of clinical status: stage I, cerebral signs (mental, behavioral); stage II, convulsive motor signs (myoclonus, incoordination, choreoathetosis, and tremors); stage III, coma, opisthotonus, decerebrate rigidity, and no responsiveness to any stimulus; stage IV, mutism, loss of cerebral cortex function, less frequent myoclonus, and diminished hypertonia. We used the Jabbour classification for the clinical staging and found that all the 21 children were in stage II. Most of children had such cognitive decline that they could not give information beyond their names or identify simple objects like a pen or watch. Detailed neuropsychologic evaluation could not be performed in these patients. We also performed MR imaging on 10 age- and sex-matched right-handed healthy controls (age range, 5–12 years, 8 boys and 2 girls) to compare age-related changes in brain parenchyma in children with SSPE. None of the controls had any neurologic or unstable medical disease nor were they on any medication. The institutional research ethics committee approved the study. Informed consent was obtained from the parents of patients and controls for MR imaging examination.

All MR imaging was performed on a 1.5T MR imaging system (Signa, GE Healthcare, Milwaukee, Wis) equipped with an actively shielded whole-body magnetic field gradient set with a maximal strength of 33 mT/m and a quadrature birdcage receive and transmit radio-frequency head coil. The conventional MR imaging protocol included a T2-weighted fast spin-echo sequence with TR/TE/echo train length/number of excitations, 6000 /200 ms/16/2; a T1-weighted spin-echo sequence with TR/TE/number of excitations, 800/14 ms/1; and a fluid-attenuated inversion recovery (FLAIR) sequence with TR/TE/ TI, 9000/89/2200 ms. Gadodiamide (Gd-DTPA-BMA, Omniscan, Amersham Health, Oslo, Norway), 0.2 mL/kg of body weight, was injected intravenously in these patients. DTI data were acquired by using a single-shot echo-planar dual spin-echo sequence with ramp sampling. The diffusion weighting b-factor was set to 1000 s/mm^2, TR ~ 8 seconds, TE ~100 ms. A total of 36 axial sections was acquired with an image matrix of 256 × 256 (following zero-filling). The diffusion tensor encoding used was the balanced rotationally invariant dodecahedral scheme with 10 uniformly distributed directions over the unit hemisphere.[15] To enhance the signal-to-noise ratio and reduce phase fluctuations, the scanner software repeated (number of excitations, 8) and temporally averaged the magnitude-constructed images. All imaging was performed in the axial plane and had identical geometric parameters: field of view, 240 × 240 mm^2; section thickness, 3 mm; section gap, 0; and number of sections, 36.

DTI Data Processing

The DTI data were processed as described in detail elsewhere.[16] Briefly, following image cropping and distortion corrections, the data were interpolated to attain isotropic voxels and decoded to obtain the tensor field for each voxel. The tensor field data were then diagonalized by using the analytic diagonalization method[15] to obtain the eigenvalues (λ_1, λ_2, and λ_3) and the 3 orthonormal eigenvectors. The tensor field data and eigenvalues were used to compute the DTI metrics such as the mean diffusivity (MD) and fractional anisotropy (FA) for each voxel.

To facilitate region of interest (ROI) placement for quantitative analysis, we displayed the DTI-derived maps and overlaid them on images with different contrasts in the 3 orthogonal planes for a visual inspection. Regional FA and MD values were obtained by placing rectangular ROIs on the genu, midbody, and splenium of the corpus callosum at the midsagittal plane in patients as well as in healthy controls. To obtain FA and MD values in the posterior limb of internal capsule, and in the frontal, parietal, and occipital lobes, we placed elliptic and rectangular ROIs at an axial plane through the third ventricle (Fig 1*C*). Elliptic ROIs were placed at the level of midbrain to obtain FA and MD values from the temporal lobe white matter. ROIs were placed on the same location in both patients with normal as well as abnormal conventional imaging. The ROI placement was based on the description of involvement of various regions on histopathology[5] and imaging.[11,17] The normal-appearing and hyperintense white matter regions of 4 cerebral lobes of the patients with SSPE on T2-weighted/FLAIR imaging were compared with those of the healthy controls. Patients with hyperintensity on T2-weighted/FLAIR imaging in brain parenchyma were considered as patients with abnormal findings on imaging. To account for the different geometric configuration of both right and left hemispheres, we compared the mean regional FA and MD values of the right hemisphere with those in the left hemisphere of healthy controls. The size of the ROI varied from 2 × 2 to 6 × 6 pixels. Areas of the genu, midbody, and splenium of the corpus callosum were measured by counting the number of pixels in each of the segments on DTI-reconstructed T2-weighted midsagittal images. The shape of the ROI for area measurements was either elliptic or rectangular or drawn freehand, depending on the sampling area within the corpus callosum. All these measurements were performed on both patients and healthy controls.

Statistical Analysis

A Student independent *t* test was performed to evaluate the regional differences in the DTI metrics and areas between patients with SSPE and healthy controls. A Student paired *t* test was also performed to evaluate the statistically significant differences between ROI measure-

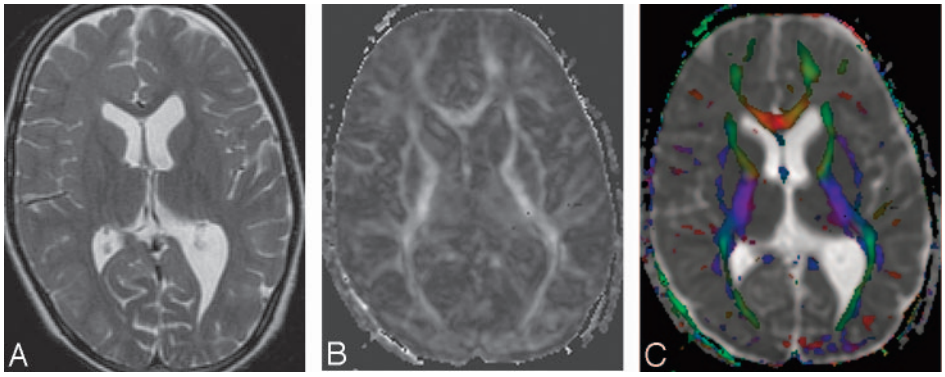

Fig 2. A 12-year-old boy with clinical findings of SSPE shows normal appearance on the T2-weighted image (*A*). FA map (*B*) shows bilateral significantly low FA values in the white matter (right frontal white matter, 0.15; left frontal white matter, 0.18; right parietal white matter, 0.16; left parietal white matter, 0.15; right occipital white matter, 0.17; left occipital white matter, 0.12). Color-coded FA fused with the ADC map (*C*) shows the abnormality more clearly.

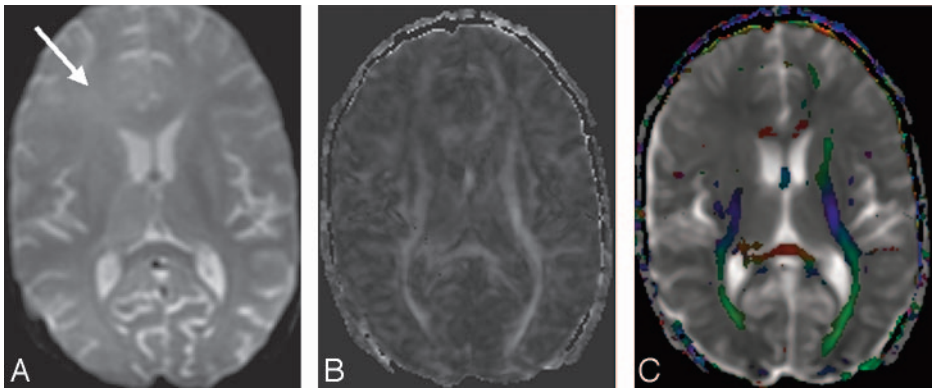

Fig 3. A 7-year-old boy with SSPE has hyperintensities on the T2-weighted (*A*) image (*arrow*) in the right frontal and parietooccipital region. The FA map (*B*) shows widespread bilateral abnormal white matter (right frontal white matter, 0.06; left frontal white matter, 0.14; right parietal white matter, 0.09; left parietal white matter, 0.13; right occipital white matter, 0.12; left occipital white matter, 0.17) and thinning of the genu and splenium of the corpus callosum. Color-coded FA fused with the ADC map (*C*) shows the abnormality more clearly.

Table 1: Summary of patient data for fractional anisotropy (FA) from the different regions of brain parenchyma collected from 10 age- and sex-matched controls and 21 patients of subacute sclerosing panencephalitis

	Corpus Callosum							
Groups	Genu	Body	Splenium	FWM	PWM	OWM	TWM	PLIC
a. Controls (n = 10)	0.55 ± 0.05	0.44 ± 0.04	0.61 ± 0.07	0.24 ± 0.04	0.25 ± 0.04	0.25 ± 0.02	0.25 ± 0.04	0.49 ± 0.06
b. PNCI (n ± 11)	0.42 ± 0.08	0.30 ± 0.08	0.43 ± 0.07	0.18 ± 0.02	0.18 ± 0.03	0.18 ± 0.04	0.19 ± 0.04	0.41 ± 0.06
c. PACI (n ± 10)	0.41 ± 0.09	0.32 ± 0.04	0.33 ± 0.11	0.15 ± 0.03	0.14 ± 0.03	0.15 ± 0.03	0.17 ± 0.02	0.39 ± 0.05
P (FA)*	P_{ab} = .00	P_{ab} = .00	P_{ab} = .00	P_{ab} = .00	P_{ab} = .00	P_{ab} = .00	P_{ab} = .00	p_{ab} = .01
	P_{ac} = .00	P_{ac} = .00	P_{ac} = .00	P_{ac} = .00	P_{ac} = .00	P_{ac} = .00	P_{ac} = .00	p_{ac} = .00
	P_{bc} = .67	P_{bc} = .44	P_{bc} = .03	P_{bc} = .00	P_{bc} = .00	P_{bc} = .00	P_{bc} = .00	p_{bc} = .48

Note:—PNCI indicates patients with normal conventional imaging; PACI, patients with abnormal conventional imaging; FWM, frontal white matter; PWM, parietal white matter; OWM, occipital white matter; TWM, temporal white matter; PLIC, posterior limb of internal capsule. Values are means ± SD.
*For FA values, P_{ab} indicates a P value a vs b; P_{bc}, P value b vs c; P_{ac}, P value a vs c.

ments in the right-to-left hemisphere in healthy controls as well as in patients with normal findings on conventional imaging. A P value of less than 0.05 was considered to be statistically significant. All statistical analyses were performed by using the Statistical Package for Social Sciences (SPSS, version 12.0, SPSS, Chicago, Ill).

Results

Qualitative Analysis

On conventional MR imaging, 10 of the 21 patients showed abnormalities. Lesions were hyperintense on T2-weighted/FLAIR images and iso- to hypointense on T1-weighted images and were distributed in the periventricular and/or subcortical white matter. In the remaining 11 patients, no abnormalities were detected on conventional MR imaging. In 9 of the 10 patients with abnormal findings on conventional imaging, lesions were distributed in the centrum semiovale (n = 7), frontal white matter (n = 7), parietooccipital white matter (n = 9), temporal white matter (n = 5), splenium (n = 2), and thalamus (n = 1). In the remaining patient, gross cerebral atrophy was present. There was no abnormal parenchymal or meningeal enhancement on postcontrast T1-weighted imaging in any of the patients. On the basis of the imaging findings, the patients were grouped into patients with normal (Fig 2*A*) and abnormal (Fig 3*A*) findings on conventional imaging for the purpose of quantitative DTI analysis. Four of 11 patients with normal findings on imaging showed motor dysfunction on clinical examination, whereas in 8 of 10 patients with abnormal findings on imaging, motor functions were impaired. These patients had gait abnormalities, spasticity, brisk deep tendon reflexes, and extensor plantar responses.

Quantitative Analysis

Mean ± standard deviation (SD) of FA and MD values in patients with SSPE and controls are listed in Tables 1 and 2.

Patients with Normal Findings on Conventional Imaging Versus Healthy Controls

FA values were significantly lower in the periventricular white matter in patients with SSPE and normal findings on conven-

Table 2: Summary of patient data for mean diffusivity (MD) from different regions of brain parenchyma collected from 10 age- and sex-matched controls and 21 patients of subacute sclerosing panencephalitis

	Corpus Callosum							
Groups	Genu	Body	Splenium	FWM	PWM	OWM	TWM	PLIC
a. Controls (n = 10)	0.80 ± 0.03	0.88 ± 0.05	0.79 ± 0.06	0.75 ± 0.05	0.70 ± 0.04	0.71 ± 0.04	0.74 ± 0.05	0.67 ± 0.03
b. PNCI (n = 11)	0.85 ± 0.05	0.96 ± 0.13	0.90 ± 0.11	0.80 ± 0.03	0.79 ± 0.06	0.78 ± 0.08	0.72 ± 0.05	0.71 ± 0.04
c. PACI (n = 10)	0.90 ± 0.24	0.94 ± 0.10	0.87 ± 0.20	0.85 ± 0.13	0.86 ± 0.17	0.87 ± 0.13	0.83 ± 0.13	0.70 ± 0.07
P (MD)*	P_{ab} = .02	P_{ab} = .11	P_{abt} = .03	P_{ab} = .00	P_{ab} = .00	P_{ab} = .00	P_{ab} = .32	P_{ab} = .07
	P_{ac} = .25	P_{ac} = .14	P_{ac} = .29	P_{ac} = .01	P_{ac} = .00	P_{ac} = .00	P_{ac} = .01	P_{ac} = .40
	P_{bc} = .45	P_{bc} = .75	P_{bc} = .73	P_{bc} = .17	P_{bc} = .15	P_{bc} = .01	P_{bc} = .00	P_{bc} = .61

Note:—PNCI indicates patients with normal conventional imaging; PACI, patients with abnormal conventional imaging; FWM, frontal white matter; PWM, parietal white matter; OWM, occipital white matter; TWM, temporal white matter; PLIC, posterior limb of internal capsule. Values are means ± SD.
*For MD values (expressed in $\times 10^{-3}$ mm^2/s), P_{ab} indicates a P value a vs b; P_{bc}, P value b vs c; P_{ac}, P value a vs c.

tional imaging (Fig 2*B*, -*C*) compared with the periventricular white matter of the controls (Fig 1*B*, -*C*) in all the cerebral lobes. The MD values were significantly higher in periventricular white matter of all the cerebral lobes except for the temporal lobe. Significantly decreased FA values were observed in the genu, midbody, and splenium of the corpus callosum and posterior limb of the internal capsule in patients compared with healthy controls. Significantly increased MD values were observed between the 2 groups in the genu and splenium of the corpus callosum. No change in MD was observed in the midbody and posterior limb of internal capsule. There was no significant change in the mean FA and MD values in the right periventricular white matter of all the cerebral lobes compared with left periventricular white matter in all patients in this group, indicating the absence of any asymmetric involvement of lobes. In addition, no significant difference in the mean FA and MD values was observed between right-to-left periventricular white matter in healthy controls.

Patients with Abnormal Findings on Imaging Versus Healthy Controls

In the patients with hyperintense lesions on T2-weighted/FLAIR imaging (Fig 3*A*), significantly reduced mean FA values and increased MD values were observed in periventricular white matter (Fig 3*B*, -*C*) of all the cerebral lobes, compared with those of healthy controls. Significantly decreased mean FA values with no change in MD values were observed in the genu, body, and splenium of the corpus callosum and posterior limb of internal capsule in patients with hyperintense lesions on T2-weighted/FLAIR imaging compared with healthy controls.

Patients with Normal Versus Abnormal Imaging Findings

Significantly decreased FA values were observed in the periventricular white matter of all the cerebral lobes in patients with abnormal findings on imaging compared with patients with normal findings on conventional imaging. Significantly increased MD values were observed only in the periventricular occipital and temporal white matter region in patients with abnormal findings on conventional imaging compared with patients with normal findings on conventional imaging. The splenium of the corpus callosum had significantly low FA values with no change in MD values compared with those of patients with normal findings on conventional imaging. No significant change in mean FA and MD values in the genu and midbody of the corpus callosum and posterior limb of internal capsule was observed in patients with abnormal findings on imaging compared with patients with normal findings on conventional imaging.

Area Measurement of Corpus Callosum

A significant decrease in the cross-sectional callosal area values in the genu (120.1 ± 25.3 mm^2), midbody (175.6 ± 47.5 mm^2), and splenium (110.3 ± 29.6 mm^2) of the corpus callosum as well as in the whole corpus callosum (435.6 ± 88.9 mm^2) in patients was observed compared with the genu (141.8 ± 27.5 mm^2), midbody (234.77 ± 31.3 mm^2), and splenium (145.0 ± 24.8 mm^2) of the corpus callosum and whole corpus callosum (612.7 ± 83.2 mm^2) in healthy controls.

Discussion

On the basis of the observations in the present study, it appears that patients with clinical stage II disease showing normal findings on conventional MR imaging have widespread microstructural changes in the white matter. Our observations of abnormal DTI measures in stage II SSPE can be explained by pathologic changes, like astrogliosis, neuronal loss and degeneration, demyelination, neurofibrillary tangles, and infiltration of inflammatory cells.[5-9] These observations are in contradiction to the conventional MR imaging findings, which are usually normal in the early stage.[2] Early imaging study findings may appear normal, with the sequential involvement of posterior parts of cerebral hemisphere as the disease progresses.[17] With time, high-signal-intensity changes in the deep white matter and severe cerebral atrophy occur on T2-weighted images.[17]

In the present study, patients with normal findings on conventional imaging (in white matter of all 4 cerebral lobes) showed significantly lower FA values than healthy controls. However, we observed significantly increased MD values in the white matter of the frontal, parietal, and occipital lobes. These observations suggest a net loss and disorganization of the structural barriers to molecular diffusion of water in the NAWM and may be explained by documented pathologic characteristics of SSPE, like demyelination, infiltration of inflammatory cells, and cytolysis of the oligodendrocytes secondary to infection by measles virus.[5,6,18] In addition, our observations are in line with the previous in vivo proton MR spectroscopy studies showing high choline/Creatine(Cr) and myoinositol/Cr ratios with normal *N*-acetylaspartate in the NAWM regions on conventional imaging.[3,12] However, significantly decreased FA with no significant change in MD in the temporal region probably reflects the early stage of the

disease, which is associated with accumulation of inflammatory cells, including macrophages, and the presence of a myelin breakdown product that could potentially restrict water molecular motion, resulting in pseudonormalization of MD.[19]

In the present study, we observed significantly reduced FA in the periventricular white matter in patients with abnormal imaging findings compared with both patients with normal conventional imaging findings and healthy controls. Similar results have been obtained on previous DTI studies in patients with other demyelinating inflammatory disease, such as multiple sclerosis, that showed significantly reduced FA values with increased MD values in the lesions compared with NAWM.[20]

The corpus callosum is associated with a different aspect of human behavior, cognition, and normal aging.[21] The rostrum and genu and midbody and splenium of the corpus callosum are associated with the parcellation units comprising frontal lobe structures and sensorimotor, midtemporal, and occipital units, respectively. In this study, regional FA values in the patients in both groups were significantly reduced in the genu, midbody, and splenium of the corpus callosum compared with those in healthy controls, suggestive of microstructural damage in the interhemispheric fibers from the hemispheric lobes that pass from the genu, midbody, and splenium of corpus callosum. The involvement of the corpus callosum was further substantiated by callosal cross-sectional-area reduction observed in the genu, midbody, and splenium. The involvement of a callosal structural component could be either due to the interruption of some interhemispheric fibers either by lesion-related secondary damage in white matter tracts of corpus callosum or by primary involvement of oligodendrocytes by the mutant viral antigen. Anlar et al[11] reported thinning of the corpus callosum and suggested that its involvement is secondary to periventricular white matter abnormality rather then primary involvement with the disease process. We speculate that the involvement of the corpus callosum is secondary to wallerian degeneration of the fibers crossing the corpus callosum because there was no focal lesion in the corpus callosum in most of the patients in this study.

Cognitive decline is the common clinical feature in patients with SSPE.[5] For example, occipital-callosal fiber tracts, passing through the splenium, play an important role in normal vision and cognitive functions.[22] The significant decrease in the corpus callosum area in patients compared with controls along with decrease in FA confirms its involvement and may be partly responsible for the cognitive decline; however, this hypothesis could not be supported from the results of the present study because detailed cognitive assessment was not performed in these patients.

Pyramidal signs and symptoms usually develop in later stages of SSPE.[5] Significantly decreased FA was observed in the posterior limb of the internal capsule in patients with normal as well as abnormal findings on imaging compared with healthy controls. However, motor dysfunction was present in only 4 patients with normal findings and in 8 patients with abnormal findings on imaging. Decreased FA in the absence of motor dysfunction suggests that it may be an early indicator of structural abnormality of these motor fibers in SSPE.

Although the current study is limited by the absence of patients with other clinical stages and lack of long-term follow-up, DTI-derived metrics obtained regionally helped in reducing the discrepancy between imaging and clinical findings. Demonstration of involvement of the parietooccipital lobe, with or without involvement of the splenium on DTI, especially in patients with normal findings on conventional imaging, may be used as an early sign of SSPE in young children with a history of childhood fever, skin rashes, and poor school performance along with behavioral changes.

Conclusion

Quantitative DTI can detect the changes in the white matter in the patients with SSPE earlier than conventional MR imaging and may be helpful in treatment planning for these patients.

References

1. Sarkar N, Gulati S, Dar L, et al. **Diagnostic dilemmas in fulminant subacute sclerosing panencephalitis (SSPE).** *Indian J Pediatr* 2004;71:365–67
2. Garg RK. **Subacute sclerosing panencephalitis.** *Postgrad Med J* 2002;78:63–70
3. Alkan A, Sarac K, Kutlu R, et al. **Early- and late-state subacute sclerosing panencephalitis: chemical shift imaging and single-voxel MR spectroscopy.** *AJNR Am J Neuroradiol* 2003;24:501–06
4. Jabbour JT, Garcia JH, Lemmi H, et al. **Subacute sclerosing panencephalitis: a multidisciplinary study of eight cases.** *JAMA* 1969;207:2248–55
5. Ohya T, Martinez AJ, Jabbour JT, et al. **Subacute sclerosing panencephalitis: correlation of clinical, neurophysiologic, and neuropathologic findings.** *Neurology* 1974;24:211–18
6. Parker JC, Klintworth GK, Graham DG, et al. **Uncommon morphologic features in subacute sclerosing panencephalitis (SSPE).** *Am J Pathol* 1970;61:275–92
7. Mandybur TI. **The distribution of Alzheimer's neurofibrillary tangles and gliosis in chronic subacute sclerosing panencephalitis.** *Acta Neuropathol (Berl)* 1990;80:307–10
8. Poon TP, Tchertkoff V, Win H. **Subacute measles encephalitis with AIDS diagnosed by fine needle aspiration biopsy: a case report.** *Acta Cytol* 1998;42:729–33
9. Cape CA, Martinez AJ, Robertson JT, et al. **Adult onset of subacute sclerosing panencephalitis.** *Arch Neurol* 1973;28:124–27
10. Brismar J, Gascon GG, Steyern KVV, et al. **Subacute sclerosing panencephalitis: evaluation with CT and MR.** *AJNR Am J Neuroradiol* 1996;17:761–72
11. Anlar B, Saatci I, Köse G, et al. **MRI findings in subacute sclerosing panencephalitis.** *Neurology* 1996;47:1278–83
12. Cakmakci H, Kurul S, Iscan A, et al. **Proton magnetic resonance spectroscopy in three subacute sclerosing panencephalitis patients: correlation with clinical status.** *Childs Nerv Syst* 2004;20:216–20
13. Jellison BA, Field AS, Medow J, et al. **Diffusion tensor imaging of cerebral white matter: a pictorial review of physics, fiber tracts, anatomy, and tumor imaging patterns.** *AJNR Am J Neuroradiol* 2004;25:356–69
14. Gupta RK, Hasan KM, Trivedi R, et al. **Diffusion tensor imaging of the developing human cerebrum.** *J Neurosci Res* 2005;81:172–78
15. Hasan KM, Parker DL, Alexander AL. **Comparison of gradient encoding schemes for diffusion-tensor MRI.** *J Magn Reson Imaging* 2001;13:769–80
16. Gupta RK, Hasan KM, Mishra AM, et al. **High fractional anisotropy in brain abscesses versus other cystic intracranial lesions.** *AJNR Am J Neuroradiol* 2005;26:1107–14
17. Tuncay R, Akman-Demir G, Gökyigit A, et al. **MRI in subacute sclerosing panencephalit.** *Neuroradiology* 1996;38:636–40
18. Hayashi M, Arai N, Satoh J, et al. **Neurodegenerative mechanisms in subacute sclerosing panencephalitis.** *J Child Neurol* 2002;17:725–30
19. Gass A, Gaa J, Schreiber WG, et al. *Assessment of the Apparent Diffusion Coefficient in Contrast-Enhancing and Chronic Lesions: The Proceedings of the International Society for Magnetic Resonance in Medicine, Sydney, Australia, April 18–24, 1998*
20. Filippi M, Cercignani M, Inglese M, et al. **Diffusion tensor magnetic resonance imaging in multiple sclerosis.** *Neurology* 2001;56:304–11
21. Abe O, Aoki S, Hayashi N, et al. **Normal aging in the central nervous system: quantitative MR diffusion-tensor analysis.** *Neurobiol Aging* 2002;23:433–41
22. Habib M, Daquin G, Pelletier J, et al. **Alexithmia as a consequence of impaired callosal function: evidence from multiple sclerosis patients and normal individuals.** In: Zaidel E, Iacoboni M, eds. *The Parallel Brain*. Cambridge, Mass: The MIT Press; 2000:415–22